II. ELECTRON OPTICS

Academic and Research Staff

Prof. John G. King
Dr. John W. Coleman
Dr. Edward H. Jacobsen

Graduate Students

Norman D. Wittels

RESEARCH OBJECTIVES AND SUMMARY OF RESEARCH

JSEP

1. High-Resolution High-Contrast Electron Optics

Joint Services Electronics Program (Contract DAAB07-74-C-0630)

John G. King, John W. Coleman

While our main objective is still the development of the Auger Emission Microscope (AEM-1),[1] we shall continue to perfect the Spherical Aberration Corrector Module (SACM),[2] and to convert some obsolete equipment into state-of-the-art apparatus for work on High Energy Electron Diffraction (HEED) and Scanning Electron Microscopy (SEM). The HEED-SEM apparatus will be used to study electrical and metallurgical properties of semiconductor compounds and devices.

Auger Emission Microscope (AEM-1)

We have essentially finished testing AEM-1, the first of three prototypes of the Auger microscope, but we continue to use it. This instrument has given us more information in some areas than we had anticipated, while in other areas it has demonstrated some new problems that were not anticipated, which must be overcome if this device is to be capable of resolving the positions and types of individual atoms in complex molecules or on surfaces.[1] Although we have not yet achieved the desired 1000 Å resolution with AEM-1, we have obtained sufficient data to begin building AEM-2 on schedule while finishing the resolution studies with AEM-1.

Spherical Aberration Corrector Module (SACM)

This work continues as the doctoral thesis research of Norman D. Wittels. During the past six months his main activity has been in theory and lens field calculations.

High-Energy Electron Diffraction (HEED) and Scanning Electron Microscopy (SEM)

We have initiated work to convert HU-10, an obsolete Transmission Electron Microscope (TEM), into a custom HEED apparatus that will permit study of semiconductor devices in active circuits as a function of controlled environmental changes. The primary data will be in the form of reflection electron diffraction patterns, obtained with a programmable electron source.

JSEP

JSEP

References

1. John W. Coleman and Steven R. Jost, "First Results with the Auger Electron Microscope (AEM-1)," Quarterly Progress Report No. 114, Research Laboratory of Electronics, M. I. T., July 15, 1974, pp. 12-21.

2. J. G. King, "Spherical Aberration Corrector Module (SACM)," Quarterly Progress Report No. 112, Research Laboratory of Electronics, M. I. T., January 15, 1974, p. 6.

JSEP

A. ELECTRON LENS FIELD CALCULATIONS

JSEP

Joint Services Electronics Program (Contract DAAB07-74-C-0630)

Norman D. Wittels, Edward H. Jacobsen, John W. Coleman

The fundamental problem in electron optical design is the selection of lens element shapes and excitations to produce a lens with the desired optical characteristics. The solution to this problem is nonunique: an arbitrarily large number of realizable lenses may possess the same optical characteristics. Attempts to constrain the solutions by requiring, say, cylindrical symmetry or time-invariant fields are not helpful, since these solutions are noncomplete: there is an infinite number of optical characteristics that cannot be satisfied by lenses of the restricted classes.[1] Some progress has been made in solving a very limited class of problems concerned with trying to improve existing lens designs,[2,3] but the direct design problem has eluded solution. Consequently, we usually solve the inverse problem, using a three-step process: (i) The lens field is calculated from the given lens element shapes and excitations. (ii) Electron trajectories are calculated from the given field and the initial conditions of the electrons. (iii) The optical characteristics are determined from considerations of selected trajectories. In electron lens design we carry out this process iteratively with different lens parameters until the calculated optical characteristics converge to the desired values. This report reviews our work on the first step of this process, the field determination.

1. Methods of Calculating Potentials

We have considered only rotationally symmetric electrostatic lenses having no volume space change, but most of the methods discussed here can be adapted to the more general cases. The lens potentials are solutions of the two-dimensional Laplace equation

$$\frac{1}{r}\frac{\partial}{\partial r}\left(r\frac{\partial\phi}{\partial r}\right)+\frac{\partial^2\phi}{\partial z^2}=0 \tag{1}$$

from which the electric fields can be obtained by partial differentiation

$$E_r=-\frac{\partial\phi}{\partial r},\quad E_z=-\frac{\partial\phi}{\partial z}. \tag{2}$$

Our problem is, How do we solve Eq. 1, subject to the boundary conditions imposed by shapes, locations, and potentials of the lens elements? Within the context of analyzing thin-film spherical aberration correctors[4] and the mirror region of the Auger microscope[5] we have explored five methods of obtaining these solutions.

JSEP

JSEP

a. Analytic Solutions

Closed analytic solutions of Eq. 1 may be found for a few electrostatic lenses.[6] Unfortunately, none of the lenses that we need to analyze can be mapped conformally into any of the simpler, solvable forms. Hence their only interest has been as test cases for comparing other methods of field calculation.

b. Assumed Solutions

It is a fundamental property of the solution of Eq. 1 that a closed, analytic expression describing the potential for all values of z along the axis suffices to determine the potential everywhere within the lens.[7] Lenses may be designed by assuming axial potentials in terms of simple sinusoidal or polynomial functions and calculating the trajectories on their bases. Once an optically suitable axial potential has been found, the off-axis potentials can be calculated and metal electrodes fashioned in the shapes of the equipotentials.[8] We have found this to be a valuable method for indicating basic lens shapes but it is not always practical or even possible to construct the calculated electrodes. Furthermore, this method reveals nothing about the effects of fringing fields, electrode misalignment, or variations in electrode voltages, so we have only used it as a first-order method.

c. Green's Function Method

By solving the classical Green's function set of integral equations,[9] the surface charges on the lens electrodes can be found as a function of the electrode potentials. The same integrals can be used to calculate the potential anywhere inside the lens from the derived charge distribution. One of the advantages of this method is that the boundary specification need not be closed, so the boundary potentials need only be specified on the electrodes. No other method discussed in this report offers this advantage. Also, the resultant surface charges are linear combinations of the contributions of the potentials of the individual electrodes. Therefore linear superposition applies: one solution of the integral equations suffices to determine the lens potentials for all possible combinations of electrode voltages. The disadvantage of this method is that virtually none of the integral equations can be solved analytically, and the space charges can only be calculated by numerical methods at a finite number of points along the electrode surfaces.

Approximate forms of the Green's function method have been used to analyze several lenses.[10] In this approach we have found that a very large number of sample points is required to achieve the necessary accuracy for lens aberration calculations (typical lenses may require many thousands of sample points). The computer time for solving so many integral equations and calculating the potentials at the trajectory points seems prohibitive.

JSEP

d. Mesh Solutions

JSEP

The solutions of Eq. 1 have the property that the potential at a point is the mean of the potential along the surface of any sphere centered on that point. This property suggests the use of "mesh" methods,[12] in which the lens is divided into a fine grid of sample points. The points on the lens boundaries retain fixed potentials, while the points of the interior potentials are adjusted successively until they converge to values approximately satisfying the mean-value principle. There have been many studies of methods to effect this relaxation process[13] and lenses have been analyzed by using potentials so derived.[14] Our studies of mesh methods have led us to the following objections.

1. While the mesh solutions converge rapidly (successive iterations do not alter the solutions appreciably), they do not converge to the correct values when compared with those lenses for which analytic solutions exist. This is most pronounced in regions near the electrodes (which are important regions in the lenses that we are examining) and emphasizes that solutions satisfying the averaging algorithms of mesh methods are <u>not</u> fundamentally solutions of Eq. 1.

2. Because the potential is calculated only at discrete points, the solution has inherent "noise" with spatial frequencies comparable to the inverse of the mesh spacings. This noise is accentuated by the processes of differentiation and interpolation which are necessary to calculate the fields at points that do not lie on the mesh.

3. Although in principle it is easy, in practice it is tedious to vary the boundary conditions or mesh point spacings. Thus it is difficult to investigate thoroughly the effects of electrode shapes and positions, and the aberrations arising from misalignments.

The simplest means of overcoming the first two objections is to construct a sequence of meshes with decreasing mesh spacings and to check for convergence of the solutions. As we have noted in the third objection, however, this causes such difficulties that we consider the method to be too cumbersome for accurate analysis.

e. Truncated Series Solution

Equation 1 has the exact solution

$$\phi(r, z) = \int_0^\infty (A_\alpha \sin \alpha z + B_\alpha \cos \alpha z)\, J_o(i\alpha r)\, d\alpha \tag{3a}$$

or equivalently

$$\phi(r, z) = \int_0^\infty \left(C_\alpha e^{\alpha z} + D_\alpha e^{-\alpha z}\right) J_o(\alpha r)\, d\alpha, \tag{3b}$$

where J_o is the zero-order Bessel function. The potential calculation is thus reduced

JSEP

JSEP to a problem of determining the functions A_α and B_α or C_α and D_α from the boundary conditions. This is analytically possible only in a few uninteresting cases whose primary utility has been to test the method. It is sometimes satisfactory to approximate Eq. 3a by a truncated series:

$$\phi(r, z) \approx \sum_{n=1}^{N} (A_n \sin \alpha_n z + B_n \cos \alpha_n z)\, I_o(\alpha_n r). \tag{4}$$

The ensuing discussion is equally applicable to Eq. 3b. The problem is thus to find an appropriate set of eigenfrequencies α_n and then to determine the coefficients A_n and B_n according to some criteria for best fit to the boundary conditions. The value of this method lies in the fact that Eq. 4 is an exact solution of Eq. 1. The eigenfrequencies and coefficients merely determine how well the solution conforms to the actual boundary conditions of the lens. Furthermore, Eq. 4 can be differentiated to calculate the field everywhere without interpolation, once the eigenfrequencies and coefficients have been determined.

The problem of choosing the eigenfrequency set is underdetermined, so it has no general solution. We have found empirically that choosing eigenfrequencies with regard to the locations of zeros and planes of symmetry and with regard to the sizes and spacings of electrodes is particularly effective. We are attempting to refine our methods of selection.

Once the eigenfrequency set has been chosen, the criterion that seems to be most effective for determining the coefficients is to least-squares fit Eq. 4 to sample points spaced along the boundary.[15] We have tried several criteria for choosing the coefficients and have found this to be the only one that converges rapidly and is stable.[16] But this rapid convergence is somewhat deceptive, since there can still be substantial errors unless the eigenfrequency set has been carefully chosen. This stresses the need for studying ways to optimize the choice. The number and the spacing of points are somewhat arbitrary except that they must completely enclose the region of the solution; the points should be concentrated in those regions where the best fit is required; and they must be everywhere at least as dense as the inverse of the highest eigenfrequency α_N. In practice, it has proved valuable to keep the number of sample points fixed while varying the eigenfrequency set to minimize the sum of the squares of the errors at the sample points. The eigenfrequency set is then held fixed and the number of sample points increased until the leading coefficients converge to stationary values. This process can be repeated until an optimal fit is achieved.

The truncated series method has been applied to a geometry similar to that of the thin-film corrector module.[4] The potentials and fields have been calculated and compare favorably with those calculated by other means. These results will be presented

JSEP in a future report.

2. Conclusions

JSEP

We have explored several methods of calculating the fields in electrostatic lenses and it appears that the truncated series method gives the most promise of helping to solve the problems of electron optical design in which we are engaged. Work will continue along this line.

References

1. An example of these limitations can be found in O. Scherzer, "Über einige Fehler von Elektronenlinsen," Z. Physik 101, 593 (1936).
2. R. W. Moses, Jr., "Lens Optimization by Direct Application of the Calculus of Variations," in P. W. Hawkes (Ed.), Image Processing and Computer-Aided Design in Electron Optics (Academic Press, London, 1973), p. 250.
3. P. W. Hawkes, "Computer-Aided Design in Electron Optics," Comput. Aided Des. 5, 200 (1973).
4. M. G. R. Thomson, "Correction of the Spherical Aberration of Electron Microscope Objective Lenses Using Transparent Foils," Quarterly Progress Report No. 102, Research Laboratory of Electronics, M.I.T., July 15, 1971, p. 6; "Achromatic Corrected Electron Foil Lenses," Quarterly Progress Report No. 103, Research Laboratory of Electronics, M.I.T., October 15, 1971, p. 1; "A Spherical-Aberration Corrector Using Electron-Transparent Conducting Foils," 31st Annual Proc. Electron Microscopy Soc. Am., New Orleans, Louisiana, August 14-17, 1973, C. J. Arceneaux (Ed.) (Claitor's Publishing Division, Baton Rouge, Louisiana, 1973), p. 262.
5. J. W. Coleman and S. R. Jost, "First Results with the Auger Electron Microscope (AEM-1)," Quarterly Progress Report No. 114, Research Laboratory of Electronics, M.I.T., July 15, 1974, p. 12; M. G. R. Thomson, "Design of an Achromatic Combined Electron Mirror and Accelerating Lens," Quarterly Progress Report No. 108, Research Laboratory of Electronics, M.I.T., January 15, 1973, p. 17.
6. M. Y. Bernard and P. Ehinger, "Theory of the Three-Electrode Lens with Thick Electrodes," Proc. 3rd Int. Conf. Electron Microscopy, V. E. Cosslett (Ed.), Royal Microscopy Soc., London (1954), p. 67; R. Rudenberg, "Electron Lenses of Hyperbolic Field Structure," J. Franklin Inst. 246, 311 (1948); E. Durand, Electrostatique, Vol. 2 (Masson, Paris, 1966); A. G. Vlasov and D. M. Krupp, "Raschet Polei Elektronnich Lenz," Izvest. Akad. Nauk SSSR, Ser. Fiz. 25, 662 (1961).
7. W. Glaser, "Elektronen- und Ionenoptik," in S. Flügge (Ed.), Handbuch der Physik, Vol. 33 (Springer Verlag, Berlin, 1956), p. 158.
8. For examples of this method of lens design, see G. N. Plass, "Electrostatic Electron Lenses with a Minimum of Spherical Aberration," J. Appl. Phys. 13, 49 (1942); J. W. Butler, "Digital Computer Techniques in Electron Microscopy," Proc. 6th International Congress for Electron Microscopy, R. Uyeda (Ed.), Vol. 1 (Maruzen, Tokyo, 1966), p. 191; J. R. Ashley, "Hybrid Computer Aided Synthesis of Thick Electrostatic Lenses," Record of 11th Symposium on Electron, Ion, and Laser Beam Technology, R. F. M. Thornley (Ed.), IEEE Publication #71C23-ED (San Francisco Press, San Francisco, 1971), p. 157; D. L. Fraser, Jr. et al., "A Computer Analysis of the Spherical Aberration of Three Electrostatic Immersion Lenses," ibid., p. 209.
9. For a general treatment of the Green's function method, see J. D. Jackson, Classical Electrodynamics (John Wiley and Sons, Inc., New York, 1962).

JSEP

JSEP 10. B. Singer and M. Braun, "Integral Equation Method for Computer Evaluation of Electron Optics," IEEE Trans., Vol. ED-17, p. 926, 1970; F. H. Read et al., "Electrostatic Cylinder Lenses I: Two Element Lenses," J. Phys. E 4, 625 (1971); F. H. Read, "'Zero Gap' Electrostatic Aperture Lenses," J. Phys. E 4, 562 (1971).

11. A. M. Thomson, "A Technique for the Simulation of Electron Optical Systems," S.B. Thesis, Department of Physics, M.I.T., 1972.

12. C. Weber, "Numerical Solution of Laplace's and Poisson's Equations and the Calculation of Electron Trajectories and Electron Beams," in A. Septier (Ed.), Focusing of Charged Particles, Vol. 1 (Academic Press, New York, 1967), p. 45.

13. See, for example, F. Lenz, "Computer-Aided Design of Electron Optical Systems," in P. W. Hawkes (Ed.), Image Processing and Computer-Aided Design in Electron Optics (Academic Press, London, 1973), p. 274. Note that simultaneous solutions can be used instead of the relaxation process (see ref. 3), but in light of the rapid convergence, we see no advantage in that method.

14. See, for example, D. DiChio et al., "Focal Properties of the Two-tube Electrostatic Lens for Large and Near-unity Voltage Ratios," Rev. Sci. Instr. 45, 559 (1974) and references contained therein.

15. F. B. Hildebrand, Introduction to Numerical Analysis (McGraw-Hill, New York, 2d ed., 1974), Sec. 7.3.

16. This conclusion is also presented and discussed in ref. 3.

B. CONDENSER UNDERFOCUS vs OVERFOCUS IN THE TRANSMISSION ELECTRON MICROSCOPE (TEM)

Joint Services Electronics Program (Contract DAAB07-74-C-0630)

Norman D. Wittels

High-resolution electron microscopy in the transmission electron microscope (TEM) requires highly coherent illumination of the specimen. This report suggests an optimal choice of the condenser lens operating conditions to achieve this coherence with minimal sacrifice of illumination intensity.

Figure II-1 is a schematic representation of the illumination system of a TEM with a double condenser system. Condenser 1 (C_1) produces a highly demagnified image of the source which becomes the object for the second condenser (C_2) lens. The size of this object, the apparent electron source for C_2, and its position along the z axis are functions of the electron gun and C_1 designs and their operating parameters; usually they are not varied during normal TEM operation.[1]

Condenser 2 (C_2), which usually has magnification near unity, images the apparent source on the specimen. The C_2 aperture limits the acceptance angle of C_2 so that the apparent source can be modeled as a disk of radius r_1 with uniform brightness β which emits into a cone of half-angle θ_1. (Typically θ_1 is on the order of milliradians.) Since the results presented here do not depend on the detailed characteristics of the C_2 lens, the lens can be modeled as an aberration-free thin lens (with coincident principal planes,

JSEP

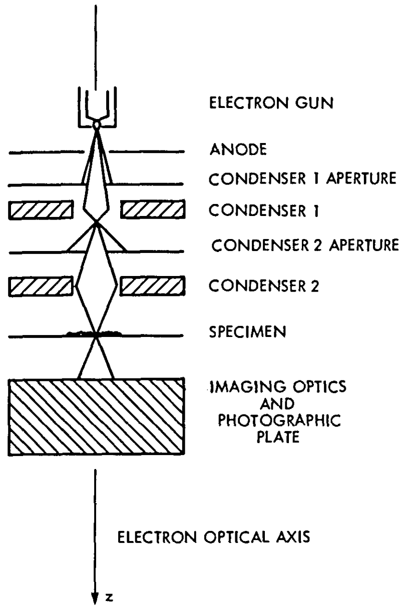

Fig. II-1.
Illumination system of a TEM.

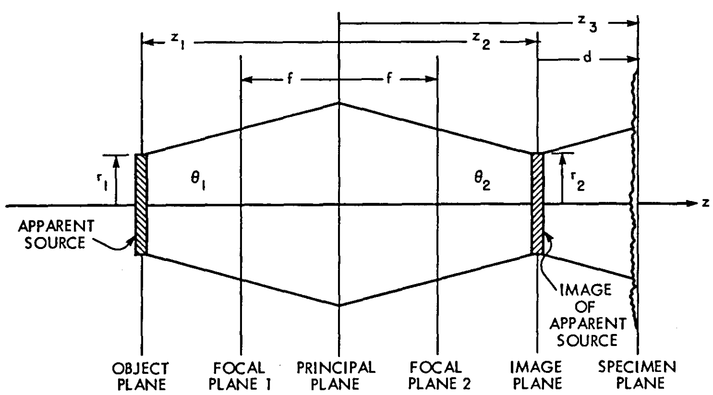

Fig. II-2. Schematic diagram of the C_2 lens.

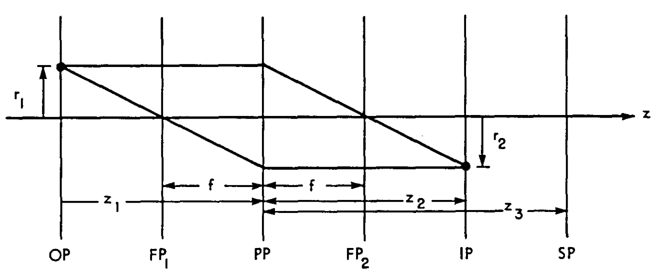

Fig. II-3. Principal rays of the C_2 lens.

JSEP and focal planes not crossed) with equal focal lengths, f. The simplified C_2 portion of the illumination system is shown in Fig. II-2.

Figure II-2 has been arranged for convenience, and f can actually be smaller or larger than z_1 or z_3. The distance z_2 is a function of f, but z_1 and z_3 are fixed by the geometry of the optical column, on the assumption that the principal planes remain fixed. Near-unity magnification implies that z_1 and z_3 are nearly equal, but the ratio z_1/z_3 will be explicitly retained in the derivation. In an axially symmetric magnetic lens, $1/f$ is proportional to $\int B_z^2\,dz$, where B_z is the axial component of the magnetic field B. Since B scales linearly with the lens current, f is proportional to $1/I^2$. We define I_o to be the lens current such that the image lies on the specimen, $z_2 = z_3$. This is called the "focus" condition and the corresponding focal length is f_o. What follows is also true if, instead of the focus condition, the "crossover" condition (the spot size at z_3 passes through a minimum) is used for the normalization. From consideration of the "principal rays," shown in Fig. II-3, we can deduce expressions for z_2 and z_3:

$$z_2 = z_1(z_1/f-1)^{-1}$$

$$z_3 = z_1(z_1/f_o-1)^{-1}.$$

The C_2 lens current can be normalized to the focus current, $\hat{I} = I/I_o$, to eliminate the focal lengths:

$$z_2 = z_1\left[\hat{I}^2(z_1/z_3+1)-1\right]^{-1}.$$

The net optical effect of the C_2 lens is to produce a real image of the source that has radius r_2,

$$r_2 = r_1(z_2/z_1) = r_1\left[\hat{I}^2(z_1/z_3+1)-1\right]^{-1},$$

and uniform brightness, and an emission half angle θ_2,

$$\theta_2 = \frac{z_1}{z_2}\theta_1 = \theta_1\left[\hat{I}^2\left(\frac{z_1}{z_3}+1\right)-1\right].$$

As shown in Fig. II-2, this image is located at distance d,

$$d = z_3 - z_2 = z_3(\hat{I}^2-1)(1+z_1/z_3)\left[\hat{I}^2(z_1/z_3+1)-1\right]^{-1},$$

away from the specimen. The factor $(\hat{I}^2-1)$ in this equation may have either sign, depending on whether the image occurs before or after the specimen. The case $(\hat{I}^2>1)$ JSEP is called "overfocus," and the case ($\hat{I}^2 < 1$) "underfocus." JSEP

Optimal specimen illumination must satisfy two requirements. First, the electron current density at the specimen must be as large as possible, since intensity limitation is almost always a problem in high-resolution operation. Second, the illumination must be coherent: its angular spread must be small compared with the acceptance angle of the optical system that images the specimen. These requirements are contradictory: the maximum current density occurs at focus where the angular divergence is θ_2, typically the same size (several milliradians) as the objective lens acceptance angle. The requirement is to find whether one should move in the direction of underfocus or overfocus to reduce the angular spread while maintaining high current density.

As a figure of merit, consider the ratio of the relative current density to the relative angular spread R,

$$R = \frac{dJ/J}{d\theta_{max}/\theta_{max}}.$$

This function, which is always positive, is to be minimized, and its value will be compared in the underfocus and overfocus regions. The criteria for comparison are as follows.

In calculating the current density and illumination half angle at a specimen point on the z axis, two cases are possible:

$$\text{Case I:} \quad \theta_2 < \tan^{-1}\left(\frac{r_2}{|d|}\right)$$

$$\text{Case II:} \quad \theta_2 > \tan^{-1}\left(\frac{r_2}{|d|}\right).$$

(The conclusions are identical for the off-axis case but the mathematical operations are not as brief.)

In Case I the apparent emitting disk (actually the image of the apparent source) is so close that the specimen is illuminated only by those electrons from the central portion of the disk. The current density[2] at the specimen is $J = \pi\beta \sin^2 \theta_2$, and the maximum angle of electron incidence is $\theta_{max} = \theta_2$. The figure of merit ratio is

$$R = \frac{\dfrac{2\pi\beta \sin\theta_2 \cos\theta_2 \, d\theta_2}{\pi\beta \sin^2\theta_2}}{\dfrac{d\theta^2}{\theta_2}} = 2\theta_2 \cot\theta_2.$$

This function is to be minimized in the vicinity of focus, so we consider its slope JSEP

JSEP

$$\frac{dR}{d\theta_2} = \frac{\sin 2\theta_2 - 2\theta_2}{\sin^2 \theta_2}.$$

Since θ_2 is positive near focus, this slope is negative. Hence R decreases in the direction of increasing θ_2 (underfocus). In Case I operation, underfocus is preferable.

In Case II the apparent emitting disk is far enough away so that electrons from all parts of it reach the specimen point. Those electrons passing through the specimen at the greatest angle come from the edge of the disk

$$\theta_{max} = \tan^{-1} \frac{r_2}{|d|} = \tan^{-1} \frac{r_1}{|\hat{I}^2 - 1|(z_1 + z_3)}.$$

The figure of merit, R, is identical to Case I, except that θ_2 is replaced by θ_{max}:

$$R = 2\theta_{max} \cot \theta_{max}.$$

Notice that there are two values of $\hat{I}$ corresponding to each value of θ_{max}: $\hat{I}^2 = 1 \pm \Delta$, where $|\Delta| < 1$. The corresponding values of R at any given θ_{max} (at any given coherence criterion) are identical. Therefore, Case II operation is symmetric with respect to underfocus and overfocus.

Using the criteria of maximum current density and minimum angular divergence in the illuminating beam, we have shown that underfocus is preferable for lens operation near the focal condition (Case I) and that there is no region of operation where overfocus is preferable (Cases I and II form a complete set). The conclusion may be drawn, with respect to these criteria and within the limitations of the model used, that condenser lens underfocus is preferable to overfocus when using a TEM for high-resolution work. This suggests a theoretical explanation for recommended practice[3] as determined empirically.

Although the conclusions presented here have been drawn from consideration of the TEM, they are applicable to all electron optical systems requiring intense, coherent illumination, including the multioptical bench developed in this laboratory.[4]

References

1. A brief but thorough description of "normal" TEM operation is found in D. Kay (Ed.), Techniques for Electron Microscopy (Blackwell Scientific Publications, Oxford, 1965), Chap. 1.

2. D. B. Langmuir, "Theoretical Limitations of Cathode-Ray Tubes," Proc. IRE 25, 977 (1937).

3. D. Kay (Ed.), op. cit., p. 20.

4. J. G. King, "Multioptical Bench," Quarterly Progress Report No. 112, Research Laboratory of Electronics, M.I.T., January 15, 1974, p. 5.

JSEP